Overexpressed p32 localized in the endoplasmic reticulum and mitochondria contributes to the negative regulation of Ca^{2+}-dependent endothelial nitric oxide synthase activity

Kwanhoon Choi

The Graduate School
Yonsei University
Department of Medicine

Overexpressed p32 localized in the endoplasmic reticulum and mitochondria contributes to the negative regulation of Ca^{2+}-dependent endothelial nitric oxide synthase activity

A Dissertation
Submitted to the Department of Medicine
and the Graduate School of Yonsei University
in partial fulfillment of the
requirements for the degree of
Doctor of Philosophy

Kwanhoon Choi

February 2021

This certifies that the Dissertation of
Kwanhoon Choi is approved.

Thesis Supervisor : **Hyun Kyo Lim**

Thesis Committee Member : **Sungwoo Ryoo**

Thesis Committee Member : **In Deok Kong**

Thesis Committee Member : **Kwang Ho Lee**

Thesis Committee Member : **Jong Taek Park**

The Graduate School
Yonsei University
February 2021

감사의 글

게으른 탓에 끝을 보지 못하던 대학원 과정이 여러 교수님과 대학원생, 학생분들의 도움으로 무사히 마무리되게 되었습니다. 한 분 한 분 찾아뵙고 감사의 말씀을 올려야 하나 그러지 못하여 송구한 마음 금할 길이 없습니다.

우선 항상 나아갈 방향을 알려주는 등대처럼 저를 이끌어주시고 지도해 주신 임현교 교수님께 무한한 감사의 말씀을 올립니다. 그리고 미숙한 연구 논문작성에도 하해와 같은 마음으로 가르침을 주신 류승우 교수님께도 무한한 감사의 말씀을 올립니다. 바쁜 일정 속에서 소중한 시간 내주셔서 자문위원으로 조언을 주신 공인덕 교수님, 이광호 교수님, 박종택 교수님께도 감사의 말씀 올립니다. 또한, 연구를 진행하고 논문작성에 큰 도움을 주신 강원대학교 구본혁 선생님 및 그 외 학생분들께도 감사의 말씀 올립니다.

그리고 제가 의사가 되고 대학원 과정을 마치도록 독려해주시고 물심양면 지원해주신 부모님께 감사드립니다.

이 논문이 나오도록 도움을 주신 모든 분께 다시 한번 감사드립니다.

2021.02

TABLE OF CONTENTS

LIST OF FIGURES

Abstract

Overexpressed p32 localized in the endoplasmic reticulum and mitochondria contributes to the negative regulation of Ca^{2+}-dependent endothelial nitric oxide synthase activity

Kwanhoon Choi

department of medicine
the graduate school, Yonsei University

(Direceted by Professor Hyun Kyo Lim)

The p32 protein plays a crucial role in the regulation of cytosolic [Ca^{2+}] ([Ca^{2+}]c) that contributes to the Ca^{2+}-dependent signaling cascade. Using an adenovirus and plasmid p32-overexpression system, we investigated the target organelles to determine if p32 was involved in the regulation of [Ca^{2+}] that may be associated with Ca^{2+}-dependent endothelial nitric oxide synthase (eNOS) activation in endothelial cells. Using electron and confocal microscopic analyses, overexpressed p32 was localized to mitochondria and the endoplasmic reticulum, and played an important role in Ca^{2+} translocation that resulted in increased [Ca^{2+}] in these organelles and reduced [Ca^{2+}]c. This decreased [Ca^{2+}]c by p32 overexpression attenuated the Ca^{2+}-dependent signaling cascade of CaMKII/AKT/eNOS phosphorylation. In aortic endothelia of wild-type mice intravenously administered adenovirus encoding the p32 gene, increased p32 levels reduced NO production and accelerated reactive oxygen species (ROS) generation. In vascular tension assay, p32 overexpression decreased acetylcholine (Ach)-induced vasorelaxation and augmented phenylephrine (PE)-dependent vasoconstriction. Notably, decreased levels of arginase II protein using siArgII was associated with downregulation of overexpressed p32 protein, which contributed to CaMKII-dependent eNOS phosphorylation at Ser1177. These results indicated that increased protein levels of p32 caused endothelial dysfunction through

attenuation of the Ca^{2+}-dependent signaling cascade, and arginase II protein participated in the stability of p32. Therefore, p32 may be a novel target to treat vascular diseases associated with endothelial disorders.

---

key words: p32, calcium concentration, endoplasmic reticulum, mitochondria, endothelial nitric oxide synthase

I. Introduction

The p32 protein, known as hyaluronan-binding protein 1 (HABP1), is exclusively localized to the mitochondria[1]. However, it is also presented on the cell surface as a receptor for globular head domains complement 1q (gC1qR), or complement 1q-binding protein (C1qbp)[2], originally recognized in the nucleus as a pre-mRNA splicing factor SF2-binding protein[3], and reported to be targeted to the golgi[4]. Exogenously epitope-tagged p32 at the N-terminus can be redirected to the endoplasmic reticulum (ER) and cell surface[5]. Functional studies have shown that p32 is required for the induction of mitochondria-dependent cell death[6,7] and p32 knockdown shifts the metabolism from oxidative phosphorylation toward aerobic glycolysis that then becomes poorly tumorogenic[8]. In addition, p32 protein contributes to the morphology of the mitochondria and ER, and to cellular metabolism and stress responses[9]. There are currently a variety of potential p32-binding partners identified. The p32 protein interacts with alpha 1B- and alpha 1D-adrenoreceptors, which control expression and cellular localization [10], and with PKCμ, which is a regulator of kinase activity and intracellular compartmentalization[11]. Then p32 protein also interacts with nuclear components such as the lamin B receptor, as a linker between the nuclear membrane and intranuclear substructures[12]. The p32 protein also binds to components of the extracellular matrix, hyaluronic acid[13], and vitronectin[14]. It is also involved in cell adhesion and motility, viral proteins, HIV Tat[15], and EBV EBNA-1[16], and exerts augmented transcriptional activation of viral proteins, bacterial surface protein, and InlB, which are necessary for bacterial invasion into mammalian cells[17].

Although endothelial nitric oxide synthase (eNOS) activity is regulated by extracellular signals, subcellular localization, and protein-protein interactions, Ca^{2+} mainly contributes to modulation of eNOS activity in these regulations. Activated Ca^{2+} bound calmodulin (Ca^{2+}/CaM) from increased cytosolic Ca^{2+} ($[Ca^{2+}]c$) levels binds to the canonical CaM-binding domain in eNOS, which promotes the alignment of the oxygenase and reductase domains of eNOS and prevents eNOS Thr495 phosphorylation. Ca^{2+}/CaM also activates Ca^{2+}/calmodulin-dependent protein kinase II (CaMKII), which participates in the phosphorylation of eNOS Ser1177 to increase NO release[18,19]. Intracellular Ca^{2+} can be transported and stored in the ER, and mitochondria. Ca^{2+} uptake by these organelles controls cellular Ca^{2+} homeostasis, regulates the oxidative phosphorylation rate and ATP synthesis, and attenuates transient $[Ca^{2+}]c$[20].

In our previous study, we reported that arginase II participates in the Ca^{2+}/CaMKII/eNOS signaling cascade by p32-dependent regulation of $[Ca^{2+}]c$. Downregulation of arginase II protein using siRNA and genetic deletion was associated with reduction of p32 protein levels, which resulted in increased $[Ca^{2+}]c$ and eNOS activation[21]. We therefore investigated the target organelles of overexpressed p32 and determined whether the p32 involved in the regulation of $[Ca^{2+}]$ was associated with Ca^{2+}-dependent eNOS activation.

II. Materials and Methods

1. Materials

N^G-nitro-L-arginine methyl ester (L-NAME) and manganese (III) tetrakis (4-benzoic acid) porphyrin chloride (MnTBAP) were purchased from Calbiochem (Darmstadt, Germany). Anti-sera against eNOS, phospho-eNOS (Ser1177 and Thr 495), phosphor-CaMKII, phospho-AKT (Ser473) and pan-actin were obtained from BD Biosciences (San Jose, CA, USA), and antiserum to p32 was from Abcam Co. (Cambridge, MA). The siRNA against arginase II (siArgII, sc-29729) and scrambled RNA (scm, sc-37007) were purchased from Santa Cruz Biotechnology (Dallas, TX). All other chemicals were obtained from Sigma-Aldrich (St. Louis, MO) unless otherwise stated.

2. Cell culture and animals

Human umbilical vein endothelial cells (HUVECs) were purchased from Cascade Biologics (Portland, OR) and maintained in Medium 200 containing low serum growth supplement according to the supplier's instructions. Male C57BL/6J wild-type (WT; Daehan Biolink, Chungbuk, Korea) were obtained at 10 weeks of age and fed a normal diet. This study adhered to the Guide for the Care and Use of Laboratory Animals (Institutional Review Board, Kangwon National University).

3. Electron microscopy (EM)

The *p32* gene was cloned into restriction sites (*AfI II/BamH I*) of the pcDNA3 connexin43-GFP-APEX2 plasmid (Addgene, Watertown, MA) for EM analysis. Human epithelical cervical carcinoma (HeLa) cells were grown on a gridded glass bottom dish (Mat-Tek, Ashland, MA). The day after seeding the cells, the p32-APEX2 gene was introduced into HeLa cells with Lipofectamine 3000 (ThermoFisher Scientific, Waltham, MA). After 16-24 hr, the cells were fixed on ice using cold 1.5 mL of fixation solution (1 % glutaraldehyde and 1 % paraformaldehyde in 0.15 M sodium cacodylate solution, pH 7.0) for 30 min. All subsequent studies were performed using pre-chilled buffers and reagents. Fixed cells were washed with 0.15 mM cold sodium cacodylate buffer, three times, on ice, and then treated for 5 min in buffer containing 50 mM glycine to quench the unreacted glutaraldehyde. Staining, using 3,3-diaminobenzidine (DAB), was initiated by adding freshly diluted 1 mg/mL DAB (Sigma-Aldrich) from a stock of the free base

dissolved in 0.1 M HCl and 10 mM H_2O_2 in phosphate-buffered saline. After 30 min, the reaction was stopped by removing the DAB solution, and the cells were washed with 0.15 M cold sodium cacodylate buffer three times on ice. Post-fixation was performed using 2 % (w/v) osmium tetroxide (OsO_4) and 1.5 % (w/v) potassium ferrocyanide in 0.1 M sodium cacodylate buffer for 1 h on ice. The cells were then rinsed three times for 10 min each in chilled distilled water, and dehydrated in a graded ethanol series (50 %, 60 %, 70 %, 80 %, 90 %, and 100 %) for 15 min each time, then it was infiltrated into EMbed-812 (Electron Microscopy Sciences, Hatfield, PA) using 1:3 (v/v), 1:1 (v/v), and 3:1 (v,v) resin and anhydrous ethanol for 1 h. The samples were exchanged with the 100 % resin and incubated overnight. The next day, the samples were exchanged again with 100% resin for 3 h before transferring the sample to fresh resin, followed by polymerization at 60 °C for 24 h. The embedded cells were cut with a diamond knife into 50 nm sections using a ultramicrotome (Leica Microsystems, Wetzlar, Germany), and images were acquired by transmission electron microscopy (TEM, Tecnai G2; Thermo Fisher Scientific) operating at 120 kV. The TEM data were acquired using the Brain Research Core Facilities at the Korea Brain Research Institute.

4. Mitochondrial fractionation

Cells and aortic segments were homogenized twice in subcellular fractionation buffer (250 mM sucrose, 20 mM HEPES, pH 7.4, 10 mM KCl, 1.5 mM MgCl2, 1 mM EDTA, 1 mM EGTA, and protease inhibitors; Roche, Basel, Switzerland) for 3 min and centrifuged at 1,000 x g for 10 min to remove cell debris and unbroken cells. The supernatants were centrifuged at 21,000 x *g* for 45 min at 4°C. The cytosolic (supernatant) and mitochondrial (pellet) fractions containing 20 μg proteins were used for subsequent western blot analyses. The purity of the fractions was measured using western blotting for HSP60 and actin, respectively.

5. Western blotting analysis

Proteins of cell lysates were dissolved in SDS/PAGE sample buffer, then resolved by 10% SDS/PAGE, and immunoblotted with a antibody (overnight at 4°C, 1:1,000 dilution). Horse radish peroxidase-conjugated antibody was detected using the enhanced chemiluminescence system (Amersham Pharmacia Biotech, Piscataway, NJ).

6. Preparation of p32 expressing adenovirus

The p32 plasmid, pCMV6-XL5, was purchased from OriGene Co. (Rockville, MD) and subcloned into restriction sites of *Bgl II/Kpn I,* of the pCMV-Tag1 plasmid. For virus generation, full-length p32 was cloned into the *BamHI* and *XhoI* sites of the pENTR-CMV vector that has attL sites for site-specific recombination with a Gateway destination vector and entry vector (Invitrogen, Carlsbad, CA). The site-specific recombination between the pENTR-CMV/p32 and the adenovirus vector, pAd/PL-DEST, was conducted using LR clonase II. WT Adp32 is an adenovirus encoding full-length human p32. The adenovirus was amplified in 293 A cells and purified using an Adeno-X^{TM} purification kit (Takara, Mountain View, CA) and the multiplicity of infection was determined using an Adeno-X^{TM} titer kit (Takara). Adp32 was used to treat HUVECs at a concentration of 1×10^6 pfu/mL. For *in vivo* mice experiments, the purified recombinant adenovirus containing 5×10^9 particles was injected in the tail vein of mice. Adenovirus only (Ad-) was used as an adenoviral control.

7. Mitochondrial Ca^{2+} ($[Ca^{2+}]m$), ER Ca^{2+} ($[Ca^{2+}]ER$), and cytosolic Ca^{2+} ($[Ca^{2+}]c$) measurements using confocal microscopy and flow cytometry

Direct assessment of $[Ca^{2+}]m$ content was peformed by an established loading procedure of the cells with Rhod-2 AM (Thermo Fisher Scientific). Briefly, the cells were loaded with 2.5 μM Rhod-2 AM at 37°C for 1 h in starvation medium. Subsequently, the cells were washed free of Rhod-2 AM and incubated in Tyrode's modified solution (150 mM NaCl, 4 mM KCl, 2 mM $CaCl_2$, 2 mM $MgCl_2$, 10 mM HEPES, and 10 mM glucose). For detection of Rhod-2 AM fluorescence, a 552 nm excitation (Ex) and a 581 nm emission (Em) filters were used. MitoTracker green FM (Thermo Fisher Scientific) was incubated at 100 nM for 1 h and imaged at 490 nm exitation and 516 nm emission. To examine the $[Ca^{2+}]ER$, ER-tracker red (5 μM, 30 min, Thermo Fisher Scientific) and Fluo-5N AM (5 μM, 1 h, Thermo Fisher Scientific) were used to obtaine images at wavelengths of 588/620 nm (Ex/Em) and 488/530 nm (Ex/Em), respectively. The $[Ca^{2+}]c$ was monitored using Fluo-4 AM (100 nM, 1 h; Thermo Fisher Scientific) at 494 nm Ex, and 506 nm Em. The intensity values were normalized according to the initial fluorescence values after subtraction of background using the Metamorph program (Molecular Probes, Eugene, OR).

$[Ca^{2+}]m$, $[Ca^{2+}]ER$, and $[Ca^{2+}]c$ were also determined using flow cytometry (FACSCalibur, BD Biosciences, San Jose, CA). The fluorescence intensity for each sample was determined using CellQuest software (BD Biosciences). The Ca^{2+} level was determined

by comparing the fold changes in the fluorescence intensities of treated cells versus control cells.

8. Measurement of NO and reactive oxygen species (ROS)

Aortic rings from 10-week-old male C57BL/6 WT mice were prepared for assays of fluorescent probe labeling of superoxide (1 μM dihydroethidine (DHE) for 5 min with 30 sec intervals) or NO (5 μM 4-amino-5-methylamino-2′,7′- difluorofluorescein diacetate (DAF-FM DA, for 5 min with 30 sec intervals). Images were acquired using an Olympus BX51 epifluorescence microscope. Fluorescence intensity was measured as previously described[22] using Metamorph software.

9. The aortic vascular tension assay

Heparin was administered 1 h before mice were sacrificed. Mice were anesthetized using isoflurane, and the thoracic aorta from the aortic root to the bifurcation of the iliac arteries was rapidly isolated and cut into 1.5 mm rings. The aortic rings were placed in ice-cold oxygenated Krebs-Ringer bicarbonate buffer (118.3 mM NaCl, 4.7 mM KCl, 1.2 mM $MgSO_4$, 1.6 mM $CaCl_2$, 25 mM $NaHCO_3$, 11.1 mM glucose; pH 7.4) and suspended between two wire stirrups (150 mm) in a myograph (Multi Myograph System; Danish Myo Technology A/S, Hinnerup Denmark; DMT-620) containing 10 mL Krebs-Ringer (95% O_2, 5% CO_2, pH 7.4, 37°C). One stirrup was connected to a three-dimensional micromanipulator, and the other to a force transducer. The aortic rings were passively stretched at 10 min intervals in increments of 100 mg to reach the optimal tone (600 mg). After the aortic rings were stretched to their optimal resting tone, the contractile response to 60 mM KCl was determined. The response to a maximal dose of KCl was used to normalize the responses to agonist across vessel rings. Dose responses to the vasoconstrictor phenylephrine (PE, 10^{-9}~10^{-5} M) were assessed, and responses to the vasodilators acetylcholine (Ach, 10^{-9}~10^{-5} M) and sodium nitroprusside (SNP, 10^{-10}~10^{-6} M) were assessed after pre-constriction with PE (10^{-5} M). To further confirm the NO-dependent vasorelaxation activity, aortic rings were treated with 1H-[1,2,4]oxadiazolo[4,3-a]quinoxalin-1-one (ODQ, 10^{-5} mol/L), a soluble guanylyl cyclase inhibitor.

10. Statistics

Each graph represents cumulative data from three independent experiments performed at

least in triplicate. Statistical significance was determined using one-way ANOVA (mean ± standard error of the mean; SEM) with a post hoc test or t-test (mean±SEM) or two-way ANOVA (mean ± standard deviation; SD) Prism 5 software (GraphPad, San Diego, CA). A value of $p < 0.05$ was considered statistically significant.

III. Results

1. p32 mainly localized to the ER and mitochondria.

To localize p32, we performed electron microscopic (EM) analysis of the p32-APEX2 system, while overexpressing p32 in HeLa cells. Fig. 1A shows that p32 was localized to the ER and mitochondria. In the untransfected cells (Figure 1Aa and 1Ab), the electron density of the mitochondria and the ER membrane was constant, but in the p32-APEX2 transfected cells (Figure 1Ac and 1Ad), strong electron density was found where DAB was precipitated, according to oxidation by the APEX2 enzyme. To further confirm these results, we prepared p32-expressing adenovirus (adp32) and infected into HUVECs. The protein amount of p32 was increased after adp32 infection (Fig. 1B) and in a time-dependent manner (Fig. 1C). Using immunocytochemical analysis, p32 after adp32 treatment was targeted at a high level to the mitochondria (Fig. 1D) and ER (Fig. 1E). Mitotracker green and concanavalin A-594 were used to indicate mitochondria and ER, respectively, showing that overexpressed p32 was localized to the Ca^{2+} storage organelles (ER and mitochondria).

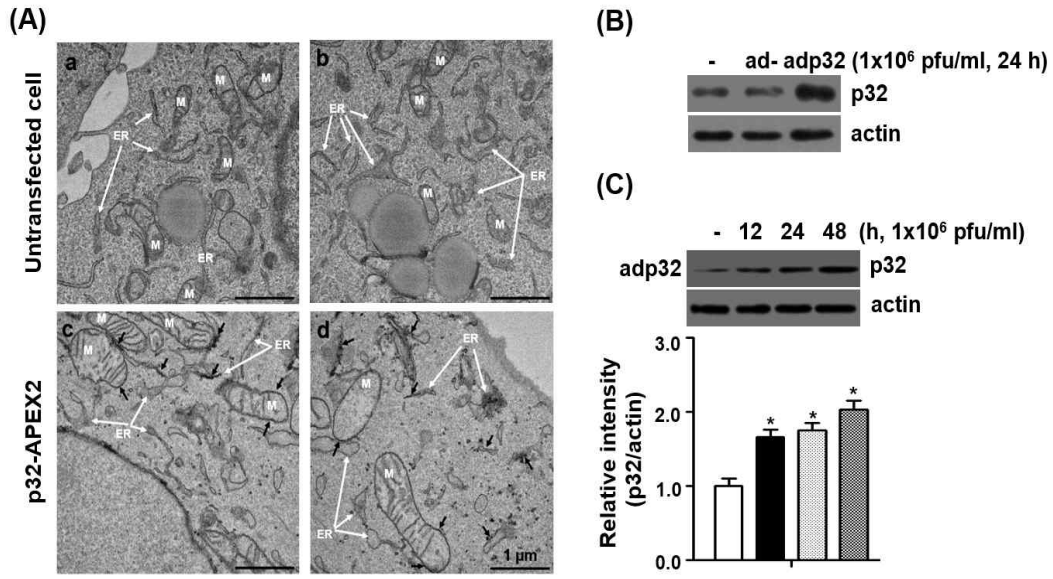

Figure 1.

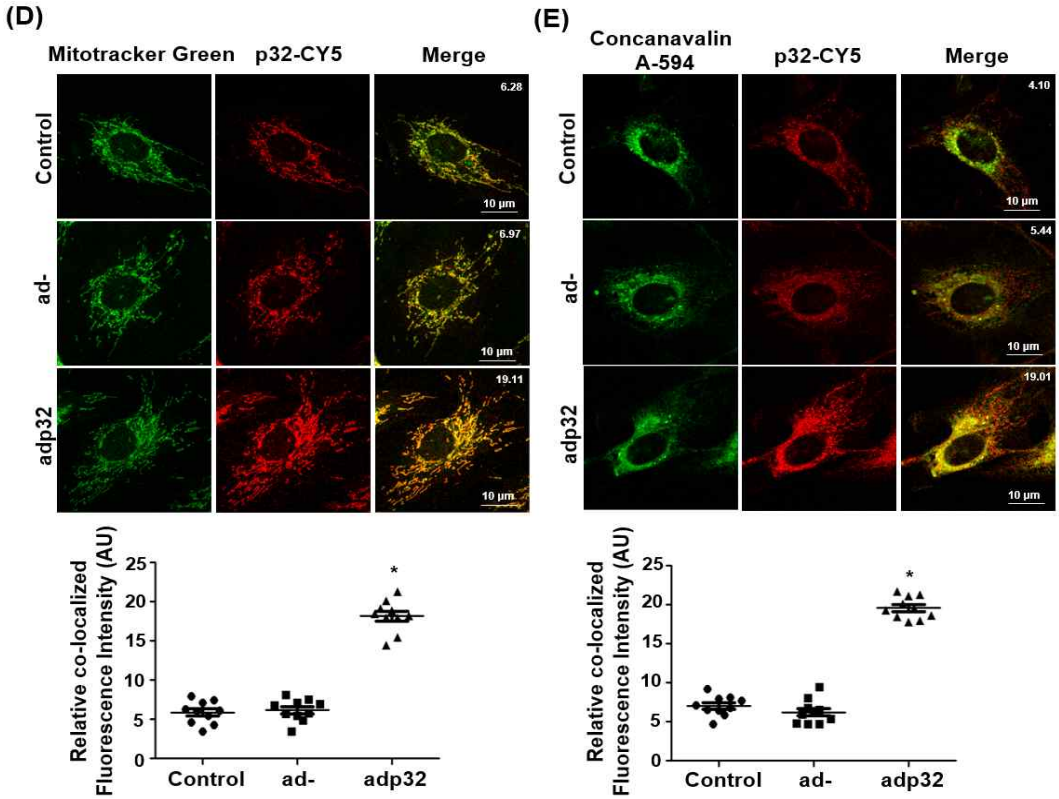

Figure 1. Overexpressed p32 targeted to the endoplasmic reticulum (ER) and mitochondria. (A) Electron microscopic analysis of the p32 localization via tagged APEX2-generated 3,3-diaminobenzidine labeling pattern. Untransfected cells showed constant staining of mitochondria and ER membrane (a and b). HeLa cells expressing the p32-APEX2 constructs showed clear densities in targeted areas. The APEX2 was targeted to the ER membrane and mitochondria membrane (black arrow, c and d). In adp32-treated HUVECs, the p32 protein level was increased (B) and p32 expression was induced in a time-dependent manner (C). *vs. untreated, $p < 0.01$, $n = 3$ experiments. Confocal microscopic images of adp32-treated HUVECs indicated that overexpressed p32 localized to both mitochondria (D) and the ER (E). Mitotracker green and concanavalin A-594 were used as indicators of mitochondria and ER, respectively.

2. p32 augmented Ca^{2+} movement from the cytosol to ER and mitochondria, resulting in decreased $[Ca^{2+}]c$.

We next tested whether increased levels of p32 localized to each organelle affected the Ca^{2+} concentration by using fluorescent dye Rhod-2 AM as a mitochondrial Ca^{2+} indicator, and Fluo-5N AM as an ER Ca^{2+} indicator. Both mitochondrial Ca^{2+} levels ($[Ca^{2+}]m$) and ER Ca^{2+} levels ($[Ca^{2+}]ER$) were significantly increased after adp32 treatment (Fig. 2A, B). We analyzed the fluorescence intensities of only Fluo-5N (Fig. 2B, top graph) and observed co-localization of Fluo-5N and ER-tracker red (Fig. 2B, bottom graph) from the microscopic images of adp32-infected HUVECs. Using fluorescence-activated cell sorting (FACS), Rhod-2 and Fluo-5N intensities were clearly moved to the right by adp32 transfection (Fig. 2C and 2D), indicating that increased p32 protein in both organelles caused an uptake of Ca^{2+}. We then determined whether adp32 changed the Ca^{2+} levels in the cytosol ($[Ca^{2+}]c$) using Fluo-4 AM. $[Ca^{2+}]c$ was decreased in adp32-treated HUVECs as observed using both microscopy (Fig. 2E) and FACS analyses (Fig. 2F). Together, the results showed that adp32-dependent p32 overexpression decreased $[Ca^{2+}]c$ by mediating Ca^{2+} uptake into the ER and mitochondria.

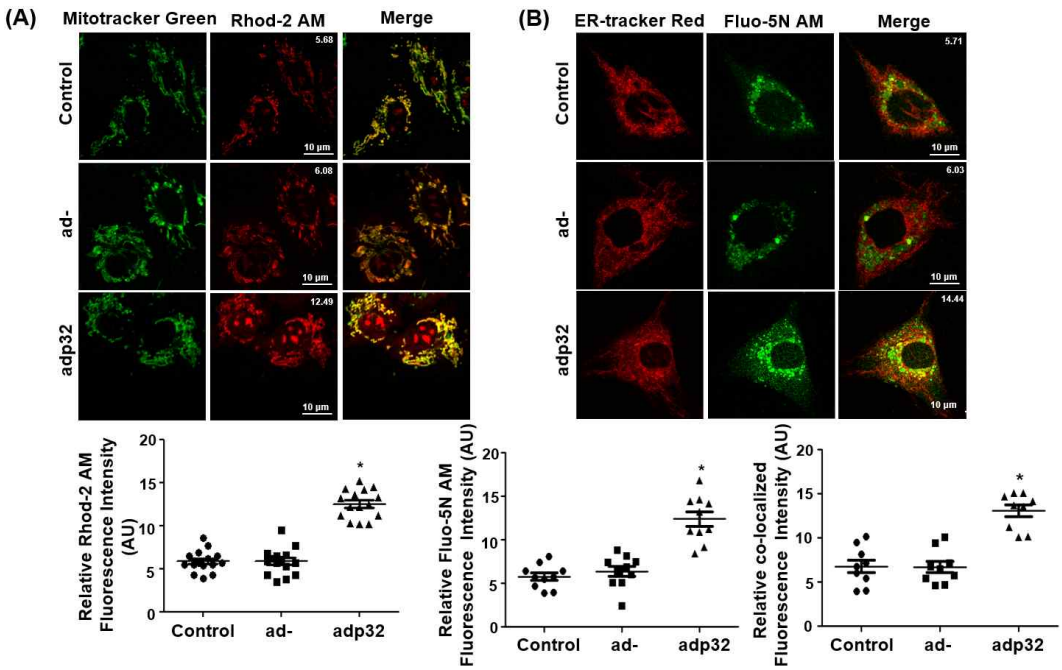

Figure 2.

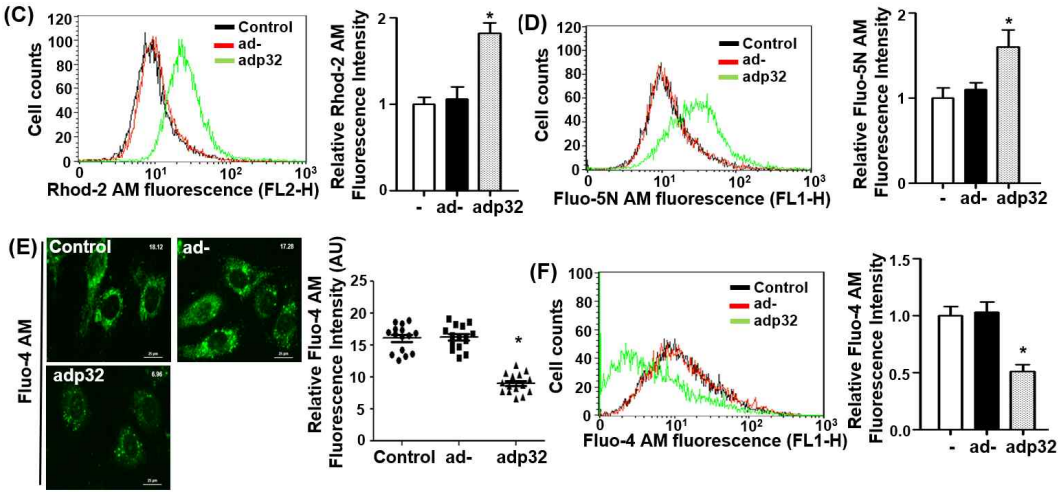

Figure 2. p32 overexpression increased [Ca^{2+}] in the ER and mitochondria. Adp32 infection induced increases in [Ca^{2+}]m (A) and [Ca^{2+}]ER (B) in microscopic images and in FACS anaysis (C and D). Rhod-2 AM was used for detecting [Ca^{2+}]m and Fluo-5N AM was used to measure [Ca^{2+}]ER. In microscopic images of [Ca^{2+}]ER, the fluorescent intensity of Fluo-5N AM was directly correlated with the colocalized fluorescent intensity of ER-tracker red and Fluo-5N AM (B, lower graph). *vs. ad-, $p < 0.01$, $n = 3$ experiments. Decreased [Ca2+]c was induced by adp32 infection in microscopic images (E) and in FACS analysis (F). *vs. ad-, $p < 0.01$, $n = 3$ experiments.

3. p32 overexpression attenuated Ca^{2+}-dependent eNOS phosphorylation and impaired endothelial function.

Because $[Ca^{2+}]c$ plays an important role in the regulation of eNOS activity through CaMKII-dependent signaling cascade in endothelial cells (ECs)[21], the Ca^{2+}-dependent signaling cascade associated with eNOS phosphorylation was next examined. The overexpression of p32 by adp32 infection attenuated the signaling cascade of CaMKII/AKT/eNOS Ser1177 phosphorylations and augmented eNOS Thr495 phosphorylation without any effect on the proteins levels (Fig. 3A). To determine the effect of adp32 on endothelial function, we intravenously injected adp32 into WT mice. Aortic vessels were isolated from the sacrificed mice to confirme that the amount of p32 protein was predominantly overexpressed in ECs, but not smooth muscle cells (Fig. 3B). In aortic endothelia infected with adp32, NO production was significantly attenuated (Fig. 3C) and ROS generation was accelerated (Fig. 3D). Using the vascular tension assay, Ach-induced vasorelaxation responses were decreased (Fig. 3E) and PE-dependent dose responses were increased (Fig. 3F), although all groups were the same in their responses to KCl (Fig. 3G) and the NO donor, SNP (Fig. 3H).

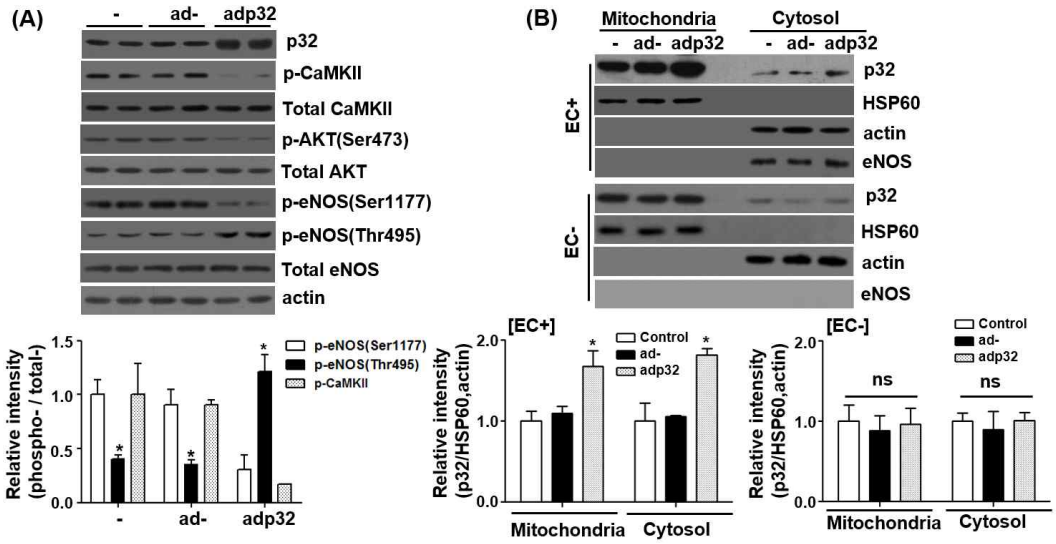

Figure 3.

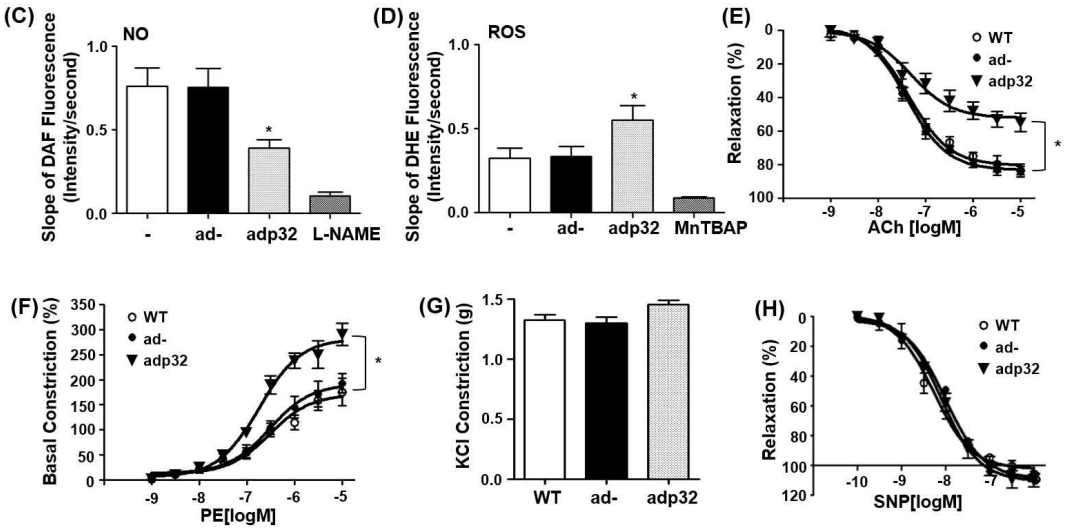

Figure 3. Adp32 infection impaired endothelial function attributing to reduced eNOS phosphorylation at Ser1177. (A) Mice injected intravenously with adp32 (5×10^9 pfu) were sacrificed after 24 h, and p32 expression was increased in aortas. Increased p32 expression decreased CaMKII/AKT/eNOS Ser1177 phosphorylations and increased eNOS phosphorylation at Thr495. Ad- had no effect on this signaling cascade. *vs. ad-, $p < 0.01$. n = 3 experiemnts. (B) p32 protein level was increased in the mitochondrial fraction of adp32-infected aortas, but the p32 protein level was not changed in the mitochondrial fraction of de-endothelialized vessels. *vs. ad-, $p < 0.01$. n = 3 experiments. ns, not significant. (C) Adp32 infection attenuated NO production and (D) accelerated ROS generation. *vs. ad-, $p < 0.01$, n = 6 aortas from three mice. Using the vascular tension assay, adp32-infected aortas had decreased responses to Ach (E) and PE-dependent vasoconstrictive responses were accelerated (F). *, ad-vs. adp32, $p < 0.01$, n = 3 mice. The KCl response (G) and SNP dose responses (H) were the same in all groups.

4. Decreased arginase II protein levels recovered adp32-dependent inactivation of eNOS.

Because the reduction of arginase II protein using siRNA against arginase II decreased the levels of p32 protein in normal physiological conditions[21], we examined whether siArgII regulated the overexpressed p32 protein levels by adp32. Interestingly, reduced arginase II protein levels after siArgII treatement resulted in decreased levels of p32 and increased CaMKII and eNOS phosphorylations in adp32-treated HUVECs (Fig. 4). These results suggested that arginase II protein was involved in the regulation of p32 stability.

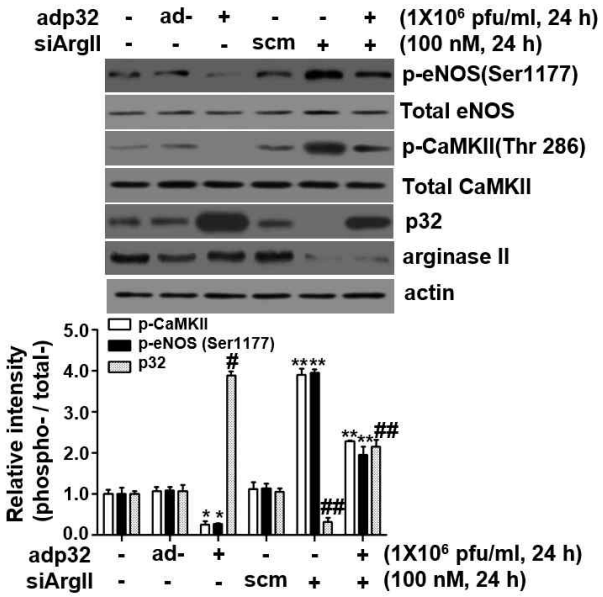

Figure 4. Arginase II protein regulated the stability of p32 protein. SiArgII was simultaneously incubated with adp32 for 24 h in HUVECs followed by determination of CaMKII and eNOS phosphorylations. Decreases in arginase II protein levels by siArgII incubation reduced p32 protein levels, resulting in increased phosphorylations of CaMKII/AKT/eNOS Ser1177. *vs. ad-, $p < 0.05$; **vs. scm, $p < 0.01$; #vs. ad-, $p < 0.01$; ##vs. scm, $p < 0.01$. n = 3 experiments.

IV. Discussion

In the present study, we showed that overexpressed p32 was preferentially localized to the ER and mitochondria, and played an important role in Ca^{2+} translocation that resulted in $[Ca^{2+}]c$ regulation. The p32 overexpression decreased $[Ca^{2+}]c$ that attenuated Ca^{2+}-dependent signaling cascade of CaMKII/AKT/eNOS phosphorylation. Using a vascular functional assay, we showed that increased amount of p32 reduced NO production and accelerated ROS generation in aortic endothelia, and reduced Ach-induced vasorelaxation and augmented PE-dependent vasoconstriction. Notably, decreased levels of arginase II protein were associated with p32 protein downregulation.

p32 is exclusively located in mitochondria, consistent with its mitochondrial targeting sequence (MTS) contained in the 73 N-terminal amino acid sequence[1,8]. However, in this study, Flag-p32 overexpression using adenovirus (ad) and plasmid was localized to the ER and mitochondria as shown in EM (Fig. 1A) and confocal microscopy (Fig. 1C and 1D). These results are consistent with a previous report that addition of an epitope tag to the N-terminus of p32 blocks the MTS, resulting in redirection because of the net negative charge of the Flag tag or because of a spacing alteration within the N-terminus[5]. Importantly, the p32 overexpression (p32-APEX2) shown in EM images was localized to ER membrane, mitochondrial membrane, and vesicles. The possibility of redirection of p32 to the ER membrane can be explained by, 1) a GFP-APEX2-dependent disturbance of p32 MTS, 2) alterations of protein interactions in the ER, 3) redirection attributed to ER stress, 4) possible membrane signals in p32, and 5) signal sequences directed to the secretory pathway[23]. Additionally, in normal physiological conditions, sip32 did not affect the change of $[Ca^{2+}]ER$, although $[Ca^{2+}]m$ was decreased (supplement Fig. 1). We therefore suggest that p32 itself was targeted to mitochondria, and not to ER, in normal conditions without the presence of a membrane signal sequence.

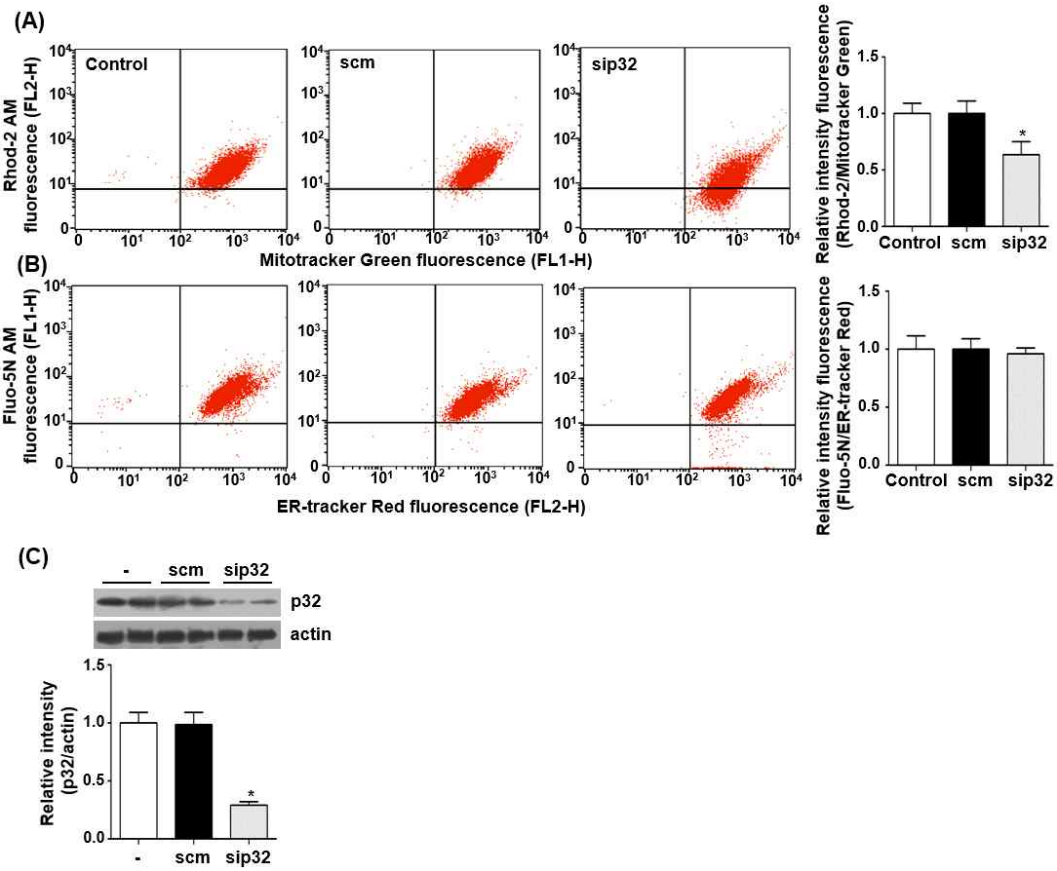

supplement Figure 1. sip32 leads to decrease in [Ca^{2+}] in only mitochondria, not in ER. In HUVECs, sip32 incubation showed reduced [Ca^{2+}]m (A), but [Ca^{2+}]ER did not changed (B). sip32 significantly reduced p32 protein level (C).

p32 is a multifunctional and multicompartmentally conserved eukaryotic protein. We previously characterized the binding ability of p32 to Ca^{2+}, and showed that spermine produced from arginase activity directly bound to p32 to farcilitate Ca^{2+} release. Knock-down of p32 resulted in reduced intracellular ATP levels, restored endothelial function in ECs, and decreased ROS generation in aortic vessels[21]. p32 protein levels were upregulated in ECs[21] and smooth muscle cells (SMCs)[24] of $ApoE^{-/-}$ mice fed an high cholesterol diet (HCD), which was associated with the impairment of the intracellular Ca^{2+} signaling cascade. We also previously showed that p32 in mitochondria played a key functional role in Ca^{2+} movement from the cytosol to mitochondria in ECs and SMCs.[21,24] As shown in Fig. 2, p32 overexpression in mitochondria and the ER consistently showed increases in Ca^{2+} concentrations in both organelles, while and $[Ca^{2+}]c$ was reciprocally reduced. These results suggested that p32 itself functioned as a channel-like protein, and not as a component of the Ca^{2+} channel complex, based on the EM images, which localized it on the membrane, as well as measurements of Ca^{2+} concentrations in the p32-targeted ER.

Because $[Ca^{2+}]c$ is an important regulator of eNOS in ECs[25], p32 overexpression induced decreases in $[Ca^{2+}]c$ that resulted in attenuated eNOS Ser1177 phosphorylation through the CaMKII/AKT signaling cascade, and enhanced eNOS Thr495 phosphorylation (Fig. 3A). These results correlated with endothelial NO production (Fig. 3C) and reduced Ach-dependent vasorelaxation (Fig. 3E), and augmented PE-induced vasoconstriction (Fig. 3F). In our previous report[21], we showed that p32 expression was upregulated in aortic endothelia of $ApoE^{-/-}$ mice fed an HCD, and increased the levels of p32 induced endotheial dysfunction in a $[Ca^{2+}]c$-dependent manner. Therefore, p32 has been identified as a new therapeutic target for vascular disorders such as atherosclerosis in which NO production is interrupted and detrimental ROS generation is promoted by endothelial dysfunction.

Arginase II, as an extrahepatic isoform, is the principal isoform in human and mouse aortic ECs, and provides L-ornithine (L-Orn) for the synthesis of polyamines associated with cell proliferation and differentiation[26,27]. Arginase II is also induced by hypoxia, lipopolysaccharide, and tumor necrosis factor α[28-30], and increased arginase II activity in ECs has recently been linked to other disorders in animal models, including aging[31], ischemic reperfusion injury[32,33], hypertension[34,35], ballon injury[36], and, atherosclerosis[22].

Because p32 plays an essential role in the regulation of $[Ca^{2+}]c$, the stability of p32 is important for the maintenance of intracellular Ca^{2+} homeostasis. We therefore propose a

novel mechanism involving arginase II being associated with p32 stability. Consistent with this possibility, reduced arginase II, by siRNA against arginase II, resulted in decreased p32 protein (Fig. 4). In addition, we found that p32 could be ubiquitinated at three lysine residues (Lys154, Lys180, and, Lys220), by using the UbPred prediction software (http://www.ubpred.org/).

In conclusion, overexpressed p32 predominantly localized to the mitochondria and ER membranes and accelerated Ca2+ movement into these organelles, which was associated with a decrease in [Ca^{2+}]c. p32 overexpression decreased the Ca^{2+}-dependent signaling cascade involved in eNOS activation and CaMKII/AKT/eNOS Ser1177 phosphorylation, and decreased NO production and increased the generation of ROS. Increased levels of p32 induced endothelial dysfunction and impaired Ach-stimulated vasorelaxation responses. Furthermore, we suggest that arginase II protein plays an important role in the maintenance of p32 stability.

References

1. Ghebrehiwet B, Lim BL, Peerschke EI, Willis AC and Reid KB: Isolation, cDNA cloning, and overexpression of a 33-kD cell surface glycoprotein that binds to the globular "heads" of C1q. J Exp Med 179: 1809-1821, 1994.
2. Krainer AR, Mayeda A, Kozak D and Binns G: Functional expression of cloned human splicing factor SF2: homology to RNA-binding proteins, U1 70K, and Drosophila splicing regulators. Cell 66: 383-394, 1991.
3. Muta T, Kang D, Kitajima S, Fujiwara T and Hamasaki N: p32 protein, a splicing factor 2-associated protein, is localized in mitochondrial matrix and is functionally important in maintaining oxidative phosphorylation. J Biol Chem 272: 24363-24370, 1997.
4. Sengupta A, Banerjee B, Tyagi RK and Datta K: Golgi localization and dynamics of hyaluronan binding protein 1 (HABP1/p32/C1QBP) during the cell cycle. Cell Res 15: 183-186, 2005.
5. van Leeuwen HC and O'Hare P: Retargeting of the mitochondrial protein p32/gC1Qr to a cytoplasmic compartment and the cell surface. J Cell Sci 114: 2115-2123, 2001.
6. Itahana K and Zhang Y: Mitochondrial p32 is a critical mediator of ARF-induced apoptosis. Cancer Cell 13: 542-553, 2008.
7. Sunayama J, Ando Y, Itoh N, et al.: Physical and functional interaction between BH3-only protein Hrk and mitochondrial pore-forming protein p32. Cell Death Differ 11: 771-781, 2004.
8. Fogal V, Richardson AD, Karmali PP, Scheffler IE, Smith JW and Ruoslahti E: Mitochondrial p32 protein is a critical regulator of tumor metabolism via maintenance of oxidative phosphorylation. Mol Cell Biol 30: 1303-1318, 2010.
9. Hu M, Crawford SA, Henstridge DC, et al.: p32 protein levels are integral to mitochondrial and endoplasmic reticulum morphology, cell metabolism and survival. Biochem J 453: 381-391, 2013.
10. Pupo AS and Minneman KP: Specific interactions between gC1qR and alpha1-adrenoceptor subtypes. J Recept Signal Transduct Res 23: 185-195, 2003.
11. Storz P, Hausser A, Link G, et al.: Protein kinase C [micro] is regulated by the multifunctional chaperon protein p32. J Biol Chem 275: 24601-24607, 2000.

12. Simos G and Georgatos SD: The lamin B receptor-associated protein p34 shares sequence homology and antigenic determinants with the splicing factor 2-associated protein p32. FEBS Lett 346: 225-228, 1994.
13. Deb TB and Datta K: Molecular cloning of human fibroblast hyaluronic acid-binding protein confirms its identity with P-32, a protein co-purified with splicing factor SF2. Hyaluronic acid-binding protein as P-32 protein, co-purified with splicing factor SF2. J Biol Chem 271: 2206-2212, 1996.
14. Lim BL, Reid KB, Ghebrehiwet B, Peerschke EI, Leigh LA and Preissner KT: The binding protein for globular heads of complement C1q, gC1qR. Functional expression and characterization as a novel vitronectin binding factor. J Biol Chem 271: 26739-26744, 1996.
15. Yu L, Zhang Z, Loewenstein PM, et al.: Molecular cloning and characterization of a cellular protein that interacts with the human immunodeficiency virus type 1 Tat transactivator and encodes a strong transcriptional activation domain. J Virol 69: 3007-3016, 1995.
16. Wang Y, Finan JE, Middeldorp JM and Hayward SD: P32/TAP, a cellular protein that interacts with EBNA-1 of Epstein-Barr virus. Virology 236: 18-29, 1997.
17. Braun L, Ghebrehiwet B and Cossart P: gC1q-R/p32, a C1q-binding protein, is a receptor for the InlB invasion protein of Listeria monocytogenes. EMBO J 19: 1458-1466, 2000.
18. Fleming I, Fisslthaler B, Dimmeler S, Kemp BE and Busse R: Phosphorylation of Thr(495) regulates Ca(2+)/calmodulin-dependent endothelial nitric oxide synthase activity. Circ Res 88: E68-75, 2001.
19. Salerno JC, Harris DE, Irizarry K, et al.: An autoinhibitory control element defines calcium-regulated isoforms of nitric oxide synthase. J Biol Chem 272: 29769-29777, 1997.
20. Lobaton CD, Vay L, Hernandez-Sanmiguel E, et al.: Modulation of mitochondrial Ca(2+) uptake by estrogen receptor agonists and antagonists. Br J Pharmacol 145: 862-871, 2005.
21. Koo BH, Hwang HM, Yi BG, et al.: Arginase II Contributes to the Ca(2+)/CaMKII/eNOS Axis by Regulating Ca(2+) Concentration Between the Cytosol and Mitochondria in a p32-Dependent Manner. J Am Heart Assoc 7: e009579, 2018.

22. Ryoo S, Gupta G, Benjo A, et al.: Endothelial arginase II: a novel target for the treatment of atherosclerosis. Circ Res 102: 923-932, 2008.
23. Peerschke EI and Ghebrehiwet B: The contribution of gC1qR/p33 in infection and inflammation. Immunobiology 212: 333-342, 2007.
24. Koo BH, Hong D, Hong HD, et al.: Arginase II activity regulates cytosolic Ca(2+) level in a p32-dependent manner that contributes to Ca(2+)-dependent vasoconstriction in native low-density lipoprotein-stimulated vascular smooth muscle cells. Exp Mol Med 51: 60, 2019.
25. Sessa WC: eNOS at a glance. J Cell Sci 117: 2427-2429, 2004.
26. Ignarro LJ, Buga GM, Wei LH, Bauer PM, Wu G and del Soldato P: Role of the arginine-nitric oxide pathway in the regulation of vascular smooth muscle cell proliferation. Proc Natl Acad Sci U S A 98: 4202-4208, 2001.
27. Li H, Meininger CJ, Hawker JR, Jr., et al.: Regulatory role of arginase I and II in nitric oxide, polyamine, and proline syntheses in endothelial cells. Am J Physiol Endocrinol Metab 280: E75-82, 2001.
28. Morris SM, Jr., Kepka-Lenhart D and Chen LC: Differential regulation of arginases and inducible nitric oxide synthase in murine macrophage cells. Am J Physiol 275: E740-747, 1998.
29. Louis CA, Reichner JS, Henry WL, Jr., et al.: Distinct arginase isoforms expressed in primary and transformed macrophages: regulation by oxygen tension. Am J Physiol 274: R775-782, 1998.
30. Collado B, Sanchez-Chapado M, Prieto JC and Carmena MJ: Hypoxia regulation of expression and angiogenic effects of vasoactive intestinal peptide (VIP) and VIP receptors in LNCaP prostate cancer cells. Mol Cell Endocrinol 249: 116-122, 2006.
31. Berkowitz DE, White R, Li D, et al.: Arginase reciprocally regulates nitric oxide synthase activity and contributes to endothelial dysfunction in aging blood vessels. Circulation 108: 2000-2006, 2003.
32. Hein TW, Zhang C, Wang W, Chang CI, Thengchaisri N and Kuo L: Ischemia-reperfusion selectively impairs nitric oxide-mediated dilation in coronary arterioles: counteracting role of arginase. FASEB J 17: 2328-2330, 2003.
33. Jung C, Gonon AT, Sjoquist PO, Lundberg JO and Pernow J: Arginase inhibition mediates cardioprotection during ischaemia-reperfusion. Cardiovasc Res 85: 147-154, 2010.

34. Zhang C, Hein TW, Wang W, et al.: Upregulation of vascular arginase in hypertension decreases nitric oxide-mediated dilation of coronary arterioles. Hypertension 44: 935-943, 2004.
35. Johnson FK, Johnson RA, Peyton KJ and Durante W: Arginase inhibition restores arteriolar endothelial function in Dahl rats with salt-induced hypertension. Am J Physiol Regul Integr Comp Physiol 288: R1057-1062, 2005.
36. Peyton KJ, Ensenat D, Azam MA, et al.: Arginase promotes neointima formation in rat injured carotid arteries. Arterioscler Thromb Vasc Biol 29: 488-494, 2009.

ABSTRACT (IN KOREAN)

소포체와 미토콘드리아에 위치하는 과발현된 p32단백질이 Ca2+에 의한 내피세포의 산화질소 합성효소 활성도를 저해하는 방향으로 조절한다.

<지도교수 임현교>

연세대학교 대학원 의학과

최관훈

p32 단백질은 세포질 내의 칼슘을 조절하는 데 중요한 역할을 하며 이는 칼슘 의존 신호전달체계에 의한다. adenovirus와 plasmid p32 과발현 시스템을 이용하여, 우리는 p32가 칼슘 조절에 관여하는지 그에 따른 칼슘에 의한 내피세포 산화질소 합성 효소와 연관이 되는지를 알아보았다.
전자현미경과 공초점 현미경을 사용하여 p32가 미토콘드리아와 소포체에 있고, 이들 기관으로 칼슘을 이동시켜 세포질 내의 칼슘 농도를 낮추는 것을 확인하였다. p32 과발현으로 감소하는 세포질 내의 칼슘은 CaMKII/AKT/eNOS인산화 칼슘 의존 신호전달체계 (Ca2+ dependent signaling cascade of CaMKII/AKT/eNOS phosphorylation)를 방해하였다. adenovirus에 p32 유전자를 표현하도록 하여 혈관 내로 주입받은 쥐들의 대동맥 내피세포에서 p32가 증가하면 산화질소의 생성이 감소하고, 활성산소의 생성이 가속화되었다. 혈관 장력 분석에서도 p32의 과발현은 아세틸콜린에 의한 혈관 이완을 감소시키고, 페닐레프린에 의한 혈관수축을 강화하였다. 특히, arginase II 단백질을 siArgII에 의해 감소시켰을 때 과발현시킨 p32 단백질이 같이 감소하였고, 이는 CaMKII에 의한 산화질소 Ser1177 인산화에 영향을 미쳤다. 이런 결과들은 p32 단백질이 증가하면 칼슘 의존 신호전달 체계가 방해받으면서 내피세포의 기능 저하가 오고, arginase II 단백질은 p32의 안정성과 연관이 있음을 보여준다. 따라서 p32는 내피세포에 의한 혈관질환이 발생할 때 중요한 목표 단백질이 될 가능성이 있다.

핵심되는 말: p32, 칼슘 농도, 소포체, 미토콘드리아, 내피세포 산화질소 합성 효소